

Supplementary Material

A Solid-State Deuterium NMR and SFG Study of the Side Chain Dynamics of Peptides Adsorbed onto Surfaces

Nicholas F. Breen¹, Tobias Weidner², Kun Li³, David G. Castner^{2,4}, and Gary P. Drobny^{1,3*}

Departments of Chemistry¹, Chemical Engineering², Physics³ and Bioengineering⁴, University of Washington, Seattle, WA 98195

Synthetic Procedures

Peptide Synthesis

LK peptides were synthesized *de novo* using standard Fmoc chemistry. Natural abundance residues were obtained in protected form from Novabiochem. L-leucine, isopropyl-d₇ (99% atom ²H) was purchased from Cambridge Isotope Laboratories and protected with Fmoc-OSu. Wang resins with L-leucine preloaded were used for all samples except L14, for which unloaded Wang resin was linked with deuterated Fmoc-Leu¹ and the substitution characterized². Peptides were synthesized on a Rainin PS3 instrument using N-methyl-2-pyrrolidone as the primary solvent and capped by reaction with acetic anhydride. After cleavage and lyophilization, purity was confirmed with mass spec and HPLC. The peptides did not require further purification.

Sample Binding and Preparation - Polystyrene

1.0 μm diameter polystyrene beads in aqueous suspension were obtained from Polysciences. An estimated binding area of 80 Å² per molecule of LKα14 (0.52 mg peptide per 1.0 ml bead suspension) was verified to form monolayer coverage on the polystyrene surface using X-ray photoelectron spectroscopy.

3 ml of bead suspension, 1.55 mg of LK peptide (in aqueous solution at 5.0 mg/ml), and 40 ml of 0.13x PBS buffer (28 mM NaCl, 7 mM KH₂PO₄/K₂HPO₄, pH 7.0) were combined in a 100 ml round bottom flask and stirred gently at room temperature for 4-12 hours, then transferred to a 50 ml centrifuge tube. The suspension was centrifuged for 2 hours at 3000×g, the supernatant removed, and the pellet resuspended in roughly 1 ml of deuterium-depleted water (Cambridge

Isotope Laboratories). This solution was transferred to a 1.5 ml microcentrifuge tube and centrifuged at 10,000×g for 10 minutes, the supernatant discarded, resuspended and centrifuged again. Following this, the pellet was resuspended a final time, flash-frozen, and lyophilized for a minimum of 3 days. UV analysis of the supernatants indicated 85-90% binding.

Sample Binding – Nanoparticles

Carboxyl-terminated, functionalized gold nanoparticles were provided as an aqueous suspension with a 400 cm²/ml surface area. Monolayer coverage was verified at the same peptide area as on polystyrene, using a bichinchoninic acid protein binding assay (Pierce MicroBCA). 50 ml of this solution was combined with 7.1 mg of LKα14 and adjusted to pH 8.0 with NH₄OH, then stirred overnight at room temperature. Centrifugation and washing were carried out as above, with the addition that non-binding Teflon tubes were used at all steps. The resulting dark paste was used directly without lyophilization.

Experimental Section

NMR Setup, Data Acquisition, and Analysis

The lyophilized polystyrene/peptide powder or the condensed nanoparticle/peptide suspension were placed in Kel-F sample holders of approximately 50 μl volume, sealed with Teflon tape, and placed in a home-built static solid-state NMR probe. Spectra were collected with a Bruker Avance II NMR spectrometer operating at a ²H frequency of 115.135 MHz. A two-pulse quadrupole echo pulse sequence with 2.65 μs π/2 pulses, a 40 μs delay between pulses, and a recycle delay of 0.35 s were used throughout. Each experiment consisted of 360,000-400,000 acquisitions. Processing was kept to 1 kHz line broadening and phase adjustment.

Deuterium lineshape simulations were obtained with a combination of the MXET1 simulation program³ and locally written Matlab code. The two-site conformational exchange has all possible rate parameters simulated by a combination of the exchange rate k_{ex} and the initial site population ratio, which indirectly incorporates the back exchange rate. To approximate the

overall motion of the peptide, a cone motion was added to the C α -C β bond, consisting of a ten-site jump evenly distributed around the surface of a cone defined by a 10° half-angle from the initial bond vector. The rate constant k_{cone} represents the jump rate (Hz) between adjacent sites on the cone model.

Simulation results were fit by inspection, and parameters varied by the smallest amounts that resulted in visible changes to the simulated spectra. For the population ratio, this was a step size of 5% (demonstrated in Figure S1a); for k_{ex} , 5×10^{-6} ; for k_{cone} , 5×10^{-4} ; and for QCC_{eff} , 1 kHz. Fits were not conducted automatically due to the difficulty of simulating proper lineshapes in the “shoulder” region at the base of the primary spectral peak, which is influenced by intermediate geometries with very low populations ($\ll 1\%$). The two-conformer model used does not take into account any additional subconformers. Since these populations are much smaller than the existing experimental error, they are expected to have no measurable impact on the parameters reported.

In all simulations, the anisotropy of the carbon-deuterium quadrupolar interaction was neglected. Comparison of simulations with and without the anisotropy taken into account established that the anisotropy was not significant at the experimental signal-to-noise. Figure S1b demonstrates one such pair of simulations, identical except for the anisotropy calculation.

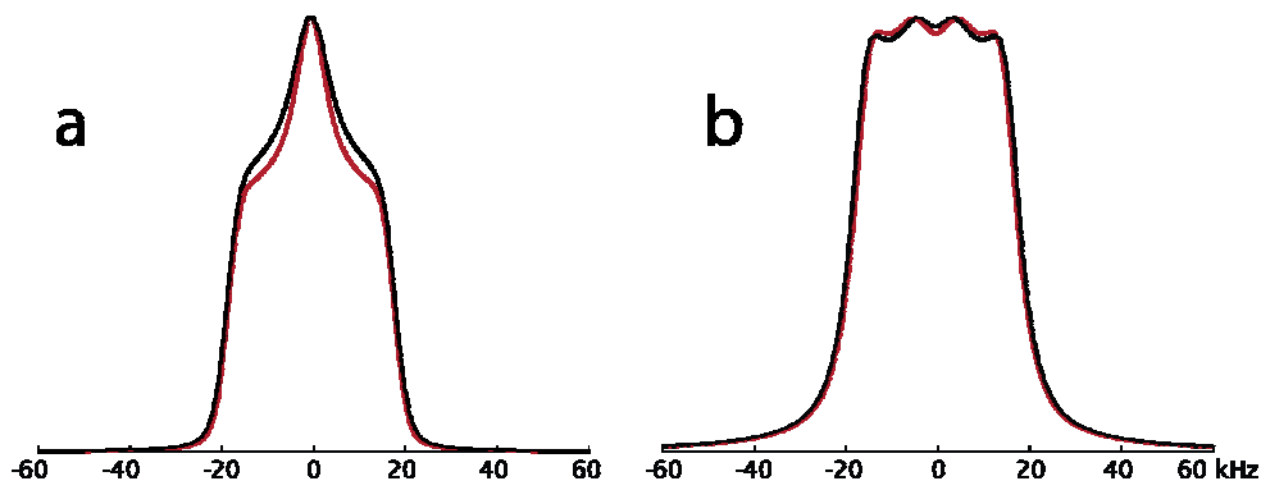


Figure S1. (a) Comparison of L8 simulations at 60:40 initial site population ratio (black line) and 55:45 (red line). All other parameters remained identical, as seen in Table 1. (b) Comparison of simulations with (black line) and without (red line) C-D quadrupolar anisotropy term included.

SFG Setup, Data Acquisition and Analysis

The SFG spectra were obtained in a co-propagating geometry by overlapping visible and tunable IR laser pulses (25 ps) in time and space at incidence angles of 60° and 54°, respectively. The visible beam with a wavelength of 532 nm was delivered by an EKSPLA Nd:YAG laser operating at 50 Hz, which was also used to pump an EKSPLA optical parametric generation/amplification and difference frequency unit based on barium borate and AgGaS₂ crystals to generate tunable IR laser radiation from 1000 - 4000 cm⁻¹. The bandwidth was 1 cm⁻¹ for the visible pump laser. The IR laser had a bandwidth of 1 cm⁻¹ in the CH stretching region and 4-6 cm⁻¹ at higher wavenumbers. Both beams were only mildly focussed and had a diameter of approximately 1 mm at the sample. The energy for each beam was 120 μJ per pulse. The SFG signal generated at the sample was then analyzed by filters and a monochromator, detected with a gated photomultiplier tube and stored in a computer. The spectra were collected with 600 shots per data point in 4 cm⁻¹ increments. All spectra were recorded in *ppp* (sum, visible, and infrared) polarization combination. The SFG spectra were normalized by a reference SFG signal generated in a ZnS crystal.

Mercaptoundecanoic acid (MUDA) SAMs were prepared on a 25 nm gold film deposited onto a CaF₂ window. Polystyrene films were prepared by spin-casting a 2 wt % solution of perdeuterated polystyrene (dPS) in toluene onto gold-covered CaF₂ windows at 3000 rpm and annealing at 120° C for 10 hours. The prepared surfaces were brought into contact with the respective solution and the surface/preptide/solution interface was probed going through the backside of the window. After a spectrum of the pristine surface in contact with a 1 x BPS buffer solution was acquired, the LKα14 peptides were injected into the liquid cell and a second spectrum was obtained. The data were normalized to a spectrum of a deuterated dodecanethiolate SAM placed into contact with deuterated water, which was acquired in the same geometry, to account for the spectral envelope of the nonresonant gold background.

The fitting routine for the SFG data⁴ used the following expression for the SFG intensity:⁵

$$I_{SFG} \propto \left| \chi^{(2)} \right|^2 = \left| \chi_{NR}^{(2)} e^{i\phi} + \sum_v \int_{-\infty}^{\infty} \frac{A_v e^{i\phi_v} e^{-[\omega_L - \omega_v / \Gamma_v]^2}}{\omega_{IR} - \omega_L + i\Gamma_L} d\omega_L \right|^2. \quad (1)$$

Here, $\chi_{NR}^{(2)}$ is the second order nonlinear susceptibility of the nonresonant background, A_ν is the strength of the ν th vibrational mode, ϕ denotes the phase of the respective mode and ω_{IR} refers to the frequency of the incident IR field. The integral is over Lorentzian lines, centered at ω_L and a width Γ_L , having a Gaussian distribution. In the fits, the Lorentzian line widths were set to 2 cm^{-1} and Γ_ν was allowed to vary since the two contributions to the total line width could not be separated within the accuracy of the measurements. Pertinent fitting results are summarized in Table S1.

Figure S2 shows the CH stretching region SFG spectrum of the peptide solution/dPS/Au interface along with a fit of eq 1 to the data. The spectrum consists of three features near 2881 cm^{-1} , 2970 cm^{-1} and 2905 cm^{-1} related to the symmetric (r^+) and asymmetric (r^-) CH_3 and the CH stretching modes of the leucine isopropyl group, respectively.⁶ The presence of these features in the spectrum indicates that the leucine side chains become ordered upon interaction with the hydrophobic dPS surface, in good agreement with the earlier work using dPS on quartz windows.⁷ A phase analysis of the symmetric CH_3 resonance reveals that this mode is in phase with the non resonant background of the gold film, showing the terminal methyl units are oriented towards the interface.⁸ Note that an analog interpretation of the asymmetric mode is complicated by a strong dependence of the relative phase on the thickness of the dPS film.⁹ Since the thickness of the dPS film used here is not exactly known, (ca. 200 nm according to literature value⁷) we have not used the latter mode for the orientation analysis.

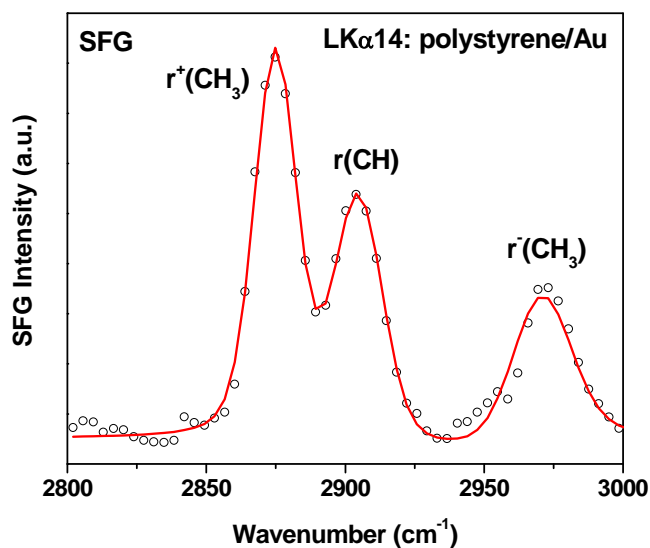


Figure S2. SFG spectrum of the LK α 14 solution/dPS interface. The spectrum shows three CH stretching modes related to the leucine side chains. The red line represents a fit of eq 1 to the data.

Table S1. SFG Spectra Peak Assignments for the Surface/Buffer Interface.

Surface	Frequency (cm ⁻¹)	Mode
MUDA SAM	2864	CH ₂ d ⁺
MUDA SAM	2897	CH-COOH d ⁺
MUDA SAM	2936	CH ₂ d ⁻
MUDA SAM	3403	OH
LK α 14 on MUDA SAM	2881	CH ₃ r ⁺
LK α 14 on MUDA SAM	2966	CH ₃ r ⁻
LK α 14 on MUDA SAM	3168	OH
LK α 14 on MUDA SAM	3262	NH
LK α 14 on dPS	2875	CH ₃ r ⁺
LK α 14 on dPS	2905	CH
LK α 14 on dPS	2970	CH ₃ r ⁻

References

- (1) Blankemeyer-Menge, B.; Nimtz, M.; Frank, R. *Tetrahedron Lett.* **1990**, *31*, 1701-1704.
- (2) Gude, M.; Ryf, J.; White, P. D. *Lett. Pept. Sci.* **2002**, *9*, 203-206.
- (3) Vold, R. R.; Vold, R. L. *Adv. Magn. Opt. Reson.* **1991**, *16*, 85-171.
- (4) Moore, F. G.; Becraft, K. A.; Richmond, G. L. *Appl. Spectrosc.* **2002**, *56*, 1575-1578.
- (5) Bain, C. D. *J. Chem. Soc., Faraday Trans.* **1995**, *91*, 1281-1296.
- (6) Watry, M. R.; Richmond, G. L. *J. Phys. Chem. B* **2002**, *106*, 12517-12523.
- (7) Mermut, O.; Phillips, D. C.; York, R. L.; McCrea, K. R.; Ward, R. S.; Somorjai, G. A. *J. Am. Chem. Soc.* **2006**, *128*, 3598-3607.
- (8) Ward, R. N.; Davies, P. B.; Bain, C. D. *J. Phys. Chem.* **1993**, *97*, 7141-7143.
- (9) (a) Lambert, A. G.; Neivandt, D. J.; Briggs, A. M.; Usadi, E. W.; Davies, P. B. *J. Phys. Chem. B* **2002**, *106*, 5461-5469. (b) McGall, S. J.; Davies, P. B.; Neivandt, D. J. *J. Phys. Chem. B* **2004**, *108*, 16030-16039.